Acta Cryst. (1984). B**40**, 582-590

Reaction Pathways from Structural Data: Dynamic Stereochemistry of Zinc(II) Compounds

BY T. P. E. AUF DER HEYDE*

Department of Chemistry, University of the Western Cape, Private Bag, Bellville 7530, *South Africa*

AND L. R. NASSIMBENI

Department of Physical Chemistry, University of Cape Town, Rondebosch 7700, *South Africa*

(*Received* 23 *August* 1983; *accepted* 8 *May* 1984)

Abstract

The structure correlation principle has been applied to the crystal structures of 33 different five-coordinate zinc complexes in order to map the mechanism for a bimolecular ligand substitution reaction at tetrahedral zinc centres. These centres are shown to undergo an association reaction leading to a slightly distorted trigonal bipyramidal (t.b.p.) intermediate, with an axial-axial angle of 163° and the axial bonds, to the leaving group and the nucleophile, lengthened by 26 pm over their standard covalent bond length. This intermediate may undergo axial dissociation, or it may pseudorotate *via* the *Berry* mechanism into a square pyramidal (s.p.) conformation. This latter branch of the reaction coordinate is shown to be a *cul-de-sac* in terms of dissociation of the intermediate, since t.b.p. conformation seems to be a prerequisite for axial departure of the leaving group. The reaction coordinates thus derived are compared to, and supported by, several *in vitro* studies.

Introduction

The kinetics of substitution reactions of tetrahedral metal complexes have evoked some interest, but their mechanism has been little studied. Basolo & Pearson (1967), in their authoritative work on inorganic reaction mechanisms, state 'Although information on substitution reactions of tetrahedral metal complexes is conspicuous largely because of its absence, the same is not true of tetrahedral compounds of non-transition elements.' In this paper we analyse structural changes at four- and five-coordinate zinc(II) compounds and interpret the results as prerequisites for an understanding of the dynamics of nucleophilic substitution and intramolecular Berry rearrangement of zinc(II) complexes. We use the technique of *structure correlation analysis* introduced by Bürgi (1973) and Dunitz (1979). To apply this method, use is made of the accurate molecular geometry derived by X-ray diffraction studies on a series of structurally related molecules. If a correlation between certain molecular parameters can be found, then this is regarded as mapping a minimum-energy path in the Born-Oppenheimer energy surface (Bürgi, Dunitz, Lehn & Wipff, 1974). With this technique, the mechanisms of various reactions have been studied, such as ligand exchange in Cd compounds (Bürgi, 1973), nucleophilic addition to carbonyl groups (Bürgi, Dunitz & Shefter, 1974), S_N2 and S_N3 substitution at tin(IV) (Britton & Dunitz, 1981), the stereoisomerization path for triphenylphosphine oxide (Bye, Schweizer & Dunitz, 1982), interaction of nucleophiles with quaternary phosphonium ions (Archer, Modro & Nassimbeni, 1981), and various other systems.

Data search and structural analysis

The Cambridge Crystallographic Data Centre (CCDC) file contains information on the space group and positional atomic coordinates for all organic and organometallic crystal structures published (Kennard, Watson, Allen, Motherwell, Town & Rodgers, 1975). A search of the CCDC file (January 1983 edition) for Zn-containing compounds revealed 379 entries. Of these, 53 were considered five-coordinate, with the ligand atoms at a distance of not more than 100 pm (100 pm ≡ 1 Å) in excess of the sum of the covalent radii of the relevant atoms. Nineteen structures were considered sterically too constrained (ligand atoms part of a porphyrin or similar system) and were rejected. The remaining 34 arrangements correspond to 33 different compounds, one being a dimer with two crystallographically independent Zn atoms. In all cases the Zn was considered to be in the +II oxidation state.

Structural formulae of the compounds are shown in Fig. 1. An initial examination of the structures showed a large variation in Zn-ligand distances and conformations ranging from trigonal bipyramidal (t.b.p.) to square pyramidal (s.p.). The analysis was carried out bearing in mind the reaction paths to be probed: nucleophilic substitution at tetrahedral Zn and possible pseudorotation.

Molecular geometries were analysed as shown in Fig. 2. In order to put all distances on a common scale, the sums of the respective covalent radii of Zn

* Author for correspondence.

0108-7681/84/060582-09$01.50

and the ligand atoms were subtracted from the actual interatomic distances yielding distance increments d_1, d_2, d_3, d_4 and d_5. Ligand atoms D_1 and D_5 were defined as those containing the largest bond angle θ_{15}, with $d_5 > d_1$. Donor atoms D_2 and D_4 were defined by the next largest angle θ_{24}, thus in turn defining D_3. Table 1 lists these increments and the atom types, while Table 2 shows the corresponding interatomic angles.

In our model we regard the attacking nucleophile as the donor atom furthest removed from Zn and, by analogy with the hypothesized t.b.p. intermediate in the S_N2 mechanism at tetrahedral carbon, the leaving group is expected to lie at 180° to this. Table 1 shows that $d_5 > d_1 > d_2$, d_3, d_4 in the majority of cases, with D_1 identified as a good leaving group, in agreement with the model.

Many of these five-coordinate structures have been imprecisely described as 'distorted square-pyramidal' or 'distorted trigonal-bipyramidal'. There is in fact a smooth transition from the t.b.p. to the s.p. conformation, as represented by the Berry mechanism in Fig. 3. In order to define rigorously the conformations of the compounds we employed the dihedral-angle method (Muetterties & Guggenberger, 1974), previously used to describe cyclic phosphoranes (Holmes, 1979). This requires the calculation of the sum of the absolute changes in dihedral angles occurring in the transition from an ideal t.b.p. to an ideal s.p. structure. We have chosen the ideal s.p. as having apical–basal bond angles (θ_{31}, θ_{32}, θ_{34}, θ_{35}) of 105°. This is the configuration obtained by placing Zn at the centre of mass of a ZnL_5 square pyramid, and is the same as that chosen by Holmes (1979). The

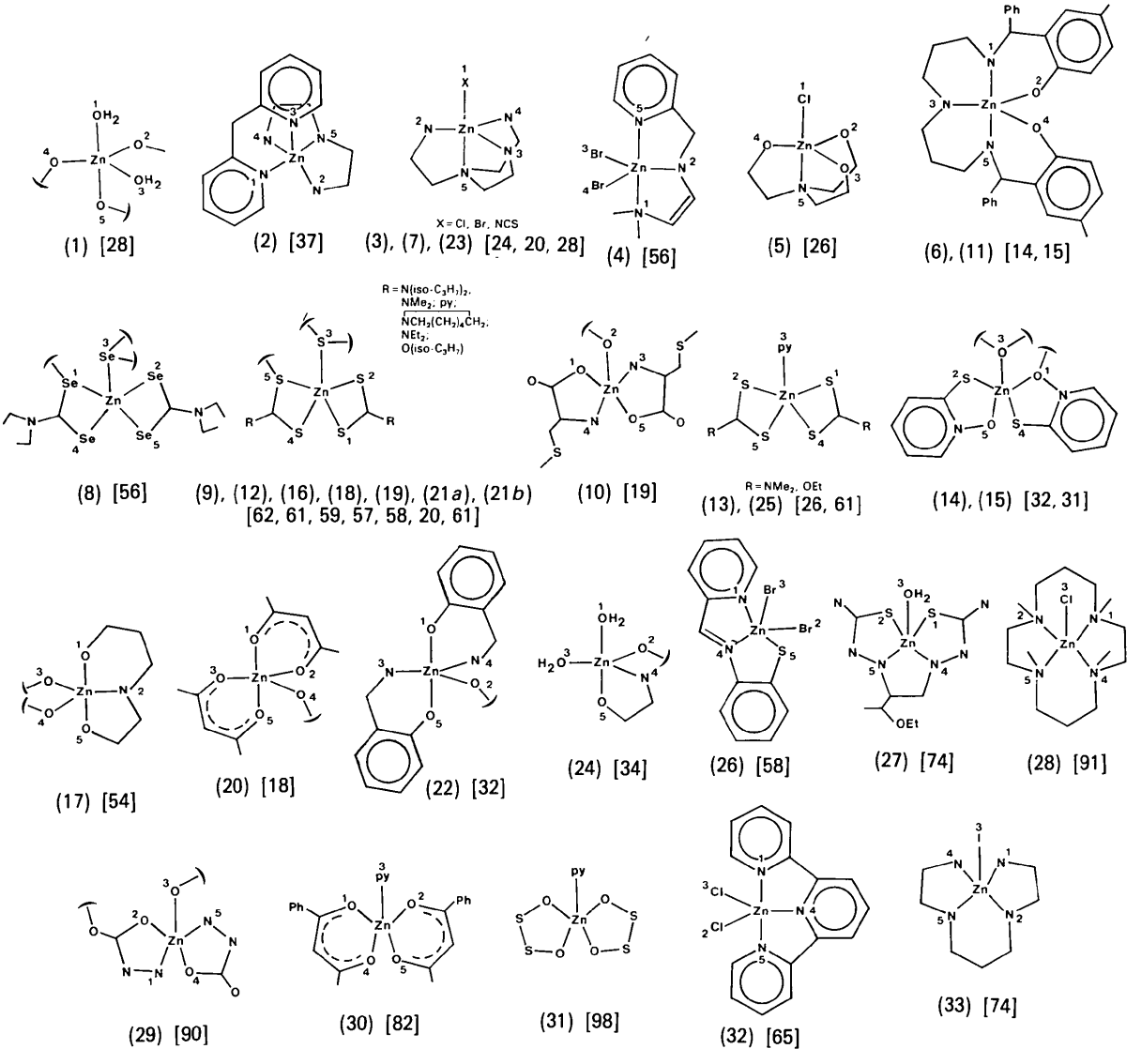

Fig. 1. Structural formulae of the compounds with sequential numbering and % distortion t.b.p. → s.p. in square brackets.

Table 1. *Atom types and distance increments d*(pm)

	D_1	D_2	D_3	D_4	D_5	d_1	d_2	d_3	d_4	d_5	CCDC acronym*
(1)	O	O	O	O	O	13	6	2	1	14	ACBZNM
(2)	N	N	N	N	N	14	9	7	7	24	AEPYZN
(3)	Cl	N	N	N	N	1	5	6	5	32	AEZNPB
(4)	N	N	Br	Br	N	23	8	−1	−2	23	BPAZHZ
(5)	Cl	O	O	O	N	−3	15	4	13	14	CEAMZN
(6)	N	O	N	O	N	11	−2	15	−3	11	CPZHZN
(7)	Br	N	N	N	N	3	11	11	11	19	DAEAZN
(8)	Se	Se	Se	Se	Se	9	−3	1	−4	55	ESECZN
(9)	S	S	S	S	S	11	−1	3	−1	47	IPTCZN
(10)	O	N	O	N	O	12	3	1	8	16	MCYSZN
(11)	N	O	N	O	N	10	−1	−2	18	10	MPZHZN
(12)	S	S	S	S	S	8	−2	2	−4	69	MTCAZN
(13)	S	S	N	S	S	25	−1	7	−2	26	MTCPZB
(14)	O	S	O	S	O	8	−4	15	−4	21	OXPTZN
(15)	O	S	O	S	O	8	−3	12	−4	22	OXPZND
(16)	S	S	S	S	S	14	−3	3	−1	56	PCDTZN10
(17)	O	N	O	O	O	−3	0	2	3	45	SALEZN
(18)	S	S	S	S	S	9	0	−1	−1	61	XMTCZN
(19)	S	S	S	S	S	9	1	3	−2	47	ZETCAM
(20)	O	O	O	O	O	3	0	4	8	13	ZNACAT10
(21*a*)	S	S	S	S	S	6	0	−4	−1	80	ZNIPXT
(21*b*)	S	S	S	S	S	2	−1	−4	1	93	
(22)	O	N	N	O	O	0	6	4	3	13	ZNMSAL10
(23)	N	N	N	N	N	3	6	4	5	28	ZNTATE10
(24)	O	N	O	O	O	16	2	1	−1	22	GLYZNS10
(25)	S	S	N	S	S	40	−6	2	−6	40	EXAPYZ
(26)	N	Br	Br	N	S	14	−2	−4	11	29	MTPYMZ
(27)	S	S	O	N	N	1	1	12	12	14	BTCBZN
(28)	N	N	Cl	N	N	18	20	−3	18	19	CTAZZN
(29)	N	O	O	O	N	7	9	6	6	7	HYZCZN
(30)	O	O	N	O	N	0	−3	7	7	10	NZBAAE10
(31)	O	O	N	O	O	4	4	4	5	5	PYZNDT
(32)	N	N	Cl	Cl	N	17	8	−2	−4	24	TPYZNC01
(33)	N	N	I	N	N	12	16	−5	13	20	ZNETAM10

* A full list of references has been deposited with the British Library Lending Division as Supplementary Publication No. SUP 39439 (4pp.). Copies may be obtained through The Executive Secretary, International Union of Crystallography, 5 Abbey Square, Chester CH1 2HU, England.

dihedral angles (δ_{ij}) were defined as the angles between the normals to the planes sharing a common edge (ij) in the idealized polyhedra as shown in Fig. 4. There are nine edges and hence nine dihedral-angle changes involved. The largest change is in δ_{24}, from 53·1° in a t.b.p. to 0° in an s.p. as listed in Table 3.

Correlations and reaction pathways

Berry pseudorotation

The sum, over all edges, of the changes in dihedral angles accompanying the t.b.p.→s.p. transition is $\sum_{ij}|\Delta|_{ij} = \sum_{ij}|\delta_{ij}(\text{t.b.p.}) - \delta_{ij}(\text{s.p.})| = 217{\cdot}9°$. If a compound C lies on the Berry rearrangement coordinate between t.b.p. and s.p. then its dihedral angles, $\delta_{ij}(C)$, are related to those of the idealized structures such that the sum of $\sum_{ij}|\delta_{ij}(C) - \delta_{ij}(\text{t.b.p.})|$ and $\sum_{ij}|\delta_{ij}(C) - \delta_{ij}(\text{s.p.})|$ is 217·9°. Table 4 lists the dihedral angles δ_{ij}.

Fig. 5 shows a plot of $217{\cdot}9° - \sum_{ij}|\delta_{ij}(C) - \delta_{ij}(\text{s.p.})|$ *vs* $\sum_{ij}|\delta_{ij}(C) - \delta_{ij}(\text{t.b.p.})|$, the Berry coordinate shown as the straight line of unit slope going

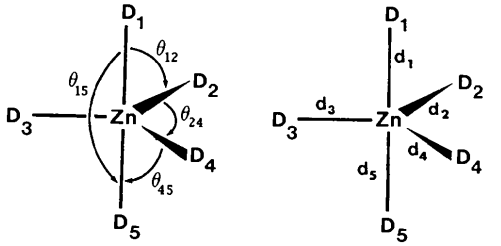

Fig. 2. Definition of molecular geometry, showing distance increments d and bond angles θ.

Table 2. *Interatomic angles* (°)

	θ_{23}	θ_{24}	θ_{34}	θ_{12}	θ_{13}	θ_{14}	θ_{52}	θ_{53}	θ_{54}	θ_{15}
(1)	116	134	110	92	83	92	88	100	86	177
(2)	123	125	112	89	89	100	81	102	82	168
(3)	113	119	113	103	102	98	79	80	79	176
(4)	112	134	114	76	101	98	75	98	95	150
(5)	115	124	114	95	106	96	82	84	78	170
(6)	118	130	112	87	91	94	91	89	88	178
(7)	118	118	118	97	97	97	83	83	83	180
(8)	115	134	108	79	105	106	89	95	71	160
(9)	104	136	117	106	110	75	69	94	92	155
(10)	123	121	116	95	99	80	80	95	91	166
(11)	124	122	113	88	98	88	90	89	87	173
(12)	106	137	111	76	114	108	94	86	66	160
(13)	116	127	117	73	96	103	102	94	73	170
(14)	105	143	112	85	96	96	100	79	82	174
(15)	106	142	111	99	96	85	82	81	96	177
(16)	106	135	115	107	110	76	69	92	91	157
(17)	121	136	89	94	118	102	76	77	79	165
(18)	104	127	123	108	112	76	67	94	86	153
(19)	112	138	108	76	105	107	94	94	70	160
(20)	119	127	111	91	95	101	88	89	77	176
(21*a*)	118	110	122	77	114	107	90	86	63	160
(21*b*)	111	118	118	108	121	77	61	92	80	146
(22)	122	125	111	93	91	99	85	96	76	173
(23)	119	118	116	97	102	99	80	81	82	177
(24)	121	139	100	96	87	91	80	94	95	175
(25)	115	129	115	72	104	97	97	104	72	152
(26)	117	133	109	96	108	76	91	96	76	148
(27)	105	144	101	118	100	81	80	94	73	153
(28)	107	150	104	90	104	84	82	102	90	154
(29)	94	152	114	80	98	98	91	105	80	156
(30)	106	147	102	106	101	88	86	98	71	154
(31)	107	153	100	86	107	88	88	100	85	153
(32)	105	143	112	73	98	101	74	102	97	145
(33)	110	137	111	82	110	94	79	104	81	145

Table 3. *Bond angles θ(°) and corresponding dihedral angles δ(°) for the idealized t.b.p. and s.p. conformations*

	θ_{15}	θ_{12}	θ_{13}	θ_{14}	θ_{52}	θ_{53}	θ_{54}	θ_{23}	θ_{24}	θ_{34}	δ_{45}	δ_{25}	δ_{14}	δ_{12}	δ_{35}	δ_{13}	δ_{23}	δ_{34}	δ_{24}
t.b.p.	180	90	90	90	90	90	90	120	120	120	101·5	101·5	101·5	101·5	101·5	101·5	53·1	53·1	53·1
s.p.	150	86	105	86	86	105	86	105	150	105	118·5	118·5	118·5	118·5	76·9	76·9	76·9	76·9	0
$\lvert\Delta\rvert_{ij}$	30	4	15	4	4	15	4	15	30	15	17	17	17	17	24·6	24·6	23·8	23·8	53·1
$\sum_{ij}\lvert\Delta\rvert_{ij}$						136										217·9			

through the origin. The scatter of the points from the coordinate may indicate the distortion of the compound geometries from the minimum-energy path associated with the Berry mechanism. We recognize, however, that whereas the geometry of the t.b.p. and its associated dihedral angles are fixed, this is not the case for the s.p. The values of the s.p. dihedral angles are dependent on the apical–basal angle chosen and the scatter of the points in Fig. 5 will also depend on this.

The Berry (1960) pseudorotation exchange mechanism is represented pictorially in Fig. 3. It involves the interconversion of two trigonal-bipyramidal structures *via* a square-pyramidal intermediate. Another mechanism proposed for such an intramolecular exchange reaction is the turnstile coordinate (Ugi, Marquarding, Klusacek, Gillespie & Ramirez, 1971). Two independent *ab initio* examinations, one on the model compound PH_5 (Altmann, Yates & Csizmadia, 1976), and the other on PF_5 (Russegger & Brickman, 1975), have shown, however, that the latter mechanism requires a considerably higher activation energy and is not a strictly different mechanistic pathway, but can be regarded as a distortion of the pentacoordinate moiety away from the minimum-energy path of the Berry process. Both studies conclude that a turnstile representation will only be realized for structurally restricted systems and the true saddle point in the interconversion of the two trigonal bipyramids corresponds to the square-pyramidal intermediate with C_{4v} symmetry.

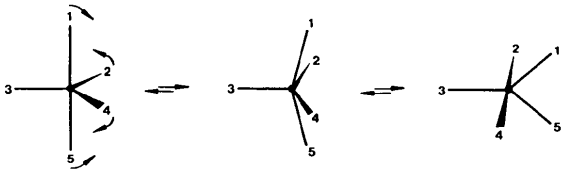

Fig. 3. Berry pseudorotation mechanism.

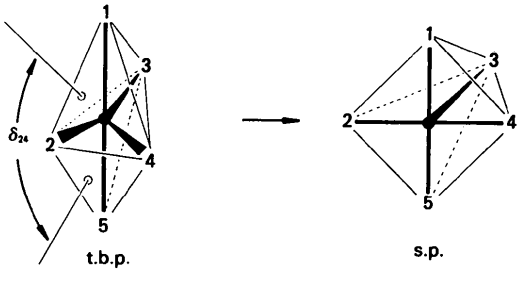

Fig. 4. Dihedral angles and edges in idealized t.b.p. and s.p. structures.

We surmise that the distortions away from the Berry coordinate, as shown by some points in Fig. 5, are possibly towards a 'turnstile' coordinate, and that these are brought about by a combination of structural restrictions imposed by the ligands.

The potential-energy hypersurface for a pentacoordinate system $[M(\text{unidentate})_5]$ has been calculated (Favas & Kepert, 1980). This maps the reaction coordinate for the interconversions between a trigonal bipyramid T_0 and two other trigonal bipyramids T_1 and T_2 *via* square-pyramidal intermediates S_1 and S_2. These conformations are shown in Fig. 6.

In their study Favas & Kepert define an axis in each of the structures T_0, T_1, T_2, S_1 and S_2 such that

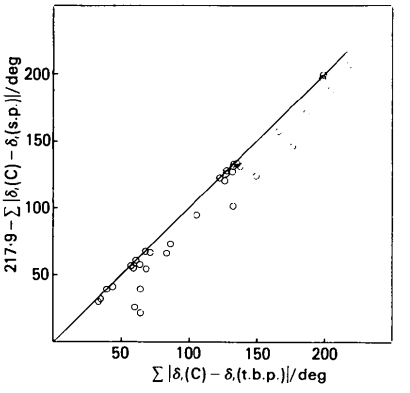

Fig. 5. Scatterplot showing smooth transition from t.b.p. to s.p. conformations, with the Berry coordinate shown as the straight line.

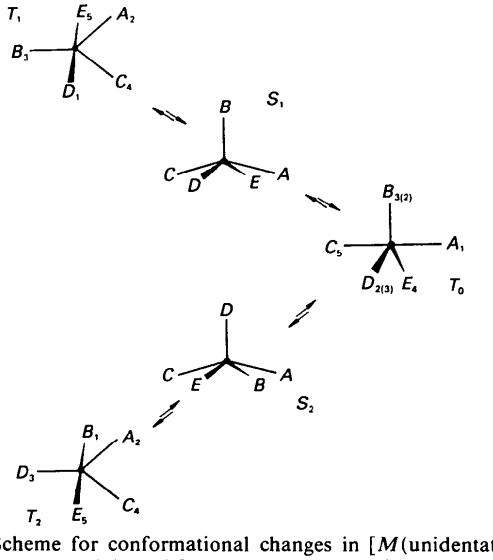

Fig. 6. Scheme for conformational changes in $[M(\text{unidentate})_5]$ systems. Adapted from Favas & Kepert (1980).

the angles φ_A, φ_B and φ_C between this axis and the bonds to each of the atoms A, B and C are all equal. φ_D and φ_E are then the angles found between the axis and the bonds to D and E respectively.

For the purposes of comparison we regarded the ligands as identical and unidentate, thus reducing the 34 different arrangements to the common system $Zn(D)_5$. Noting that the angles φ_D and φ_E are defined within the plane BDE, we chose to project the reaction coordinate derived from the crystal structures on to that plane, by plotting θ_{BD} against θ_{BE}. By superimposing our choice of ligand numbering on the conformations T_0, T_1 and T_2, the parameters θ_{BE} and θ_{BD} were calculated and plotted on Fig. 7. The similarity between the features of the potential-energy surface obtained from the point-charge model and that plotted from the crystal structures is both striking and gratifying.

The foregoing discussion has shown the possibility of the five-coordinate Zn complex undergoing pseudorotation. Recalling that the t.b.p. conformation may represent the intermediate in the S_N2 mechanism:

$$D_5 + L_3ZnD_1 \rightarrow \{D_5 \ldots ZnL_3 \ldots D_1\} \rightarrow D_5ZnL_3 + D_1,$$

where $L = D_2$, D_3, D_4, we wished to characterize this intermediate further.

The distortions which arise in the complexes as the entering nucleophile D_5 approaches the Zn^{2+} ion are tabulated in Table 4 and shown on Fig. 8.

The plot of d_5 *vs* % distortion from t.b.p. to s.p. shows that for $d_5 > 30$ pm the conformation of the $D_5 \ldots L_3ZnD_1$ system is displaced approximately 57% towards s.p. Structure (21*a*) ($d_5 = 80$ pm, 20%) is distorted from the mean line of attack by the close presence of a sixth potential donor ligand. The geometry of this structure also lies furthest away from the Berry coordinate shown in Fig. 4.

Table 4. *Dihedral angles* (°) *found in the complexes and their % distortion t.b.p.→s.p.*

	δ_{45}	δ_{25}	δ_{14}	δ_{12}	δ_{35}	δ_{13}	δ_{23}	δ_{34}	δ_{24}	%
(1)	109	112	103	107	91	98	56	57	39	28
(2)	106	112	98	103	89	77	50	65	38	37
(3)	102	100	111	107	99	73	53	46	45	24
(4)	107	109	106	108	89	90	53	82	25	56
(5)	103	101	111	111	91	99	58	57	39	26
(6)	102	108	103	106	100	99	51	58	43	14
(7)	99	99	108	108	99	72	50	50	50	20
(8)	115	112	106	118	89	86	58	64	19	56
(9)	113	114	121	107	89	90	69	61	13	62
(10)	100	108	107	104	98	98	56	55	41	19
(11)	105	107	103	104	97	99	52	58	45	15
(12)	119	106	114	119	85	88	64	58	15	61
(13)	116	103	104	115	98	98	53	52	36	26
(14)	111	99	111	110	90	97	66	55	43	32
(15)	104	108	114	106	92	95	62	60	42	31
(16)	111	114	121	109	89	89	65	60	15	59
(17)	101	120	109	127	89	88	49	72	21	54
(18)	114	111	121	103	88	84	69	54	17	57
(19)	116	111	108	119	90	89	61	65	17	58
(20)	105	103	102	110	93	100	54	59	43	18
(21*a*)	113	97	104	111	109	105	54	47	35	20
(21*b*)	111	114	118	106	84	82	63	57	14	61
(22)	104	107	99	108	91	78	57	60	42	32
(23)	100	102	105	108	80	76	49	54	49	28
(24)	103	120	103	114	92	96	46	64	37	34
(25)	119	111	111	119	88	88	59	59	14	61
(26)	109	111	109	112	87	86	78	56	18	58
(27)	115	117	121	114	69	89	82	56	13	74
(28)	117	117	115	118	79	79	74	76	5	91
(29)	119	115	125	115	81	76	76	71	4	90
(30)	119	116	117	113	73	88	80	66	8	82
(31)	119	122	116	119	75	78	75	78	0	98
(32)	113	114	110	113	84	86	56	85	14	65
(33)	110	111	110	113	82	87	73	81	8	74

From Fig. 8 we may classify the compounds into three broad types: (i) those intermediate between t.b.p. and s.p., for which $d_5 > 30$ pm; (ii) those distorting towards s.p. and (iii) those distorting towards t.b.p. Groups (i) and (iii) were considered together and examined as previously described for five-coordinate Cd complexes (Bürgi, 1973).

Substitution mechanism

The compounds were treated as distorted t.b.p.'s and we sought a correlation between the displacement

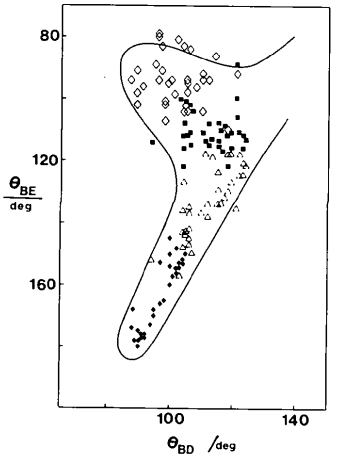

Fig. 7. Superposition of experimentally found conformations on the potential-energy surface.

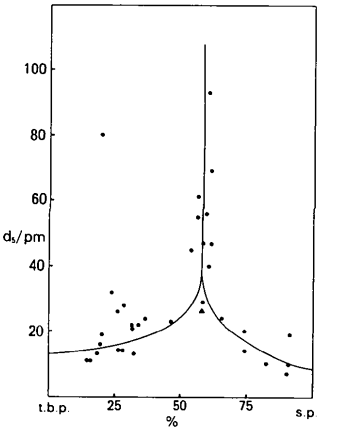

Fig. 8. Variation of distortion from t.b.p. to s.p. conformation *versus* distance of approaching nucleophile. The triangle corresponds to the conformation with $d_5 = 26$ pm and $\theta_{15} = 163°$, the average angle of nucleophilic attack.

z (Table 5) of the Zn^{2+} ion from the equatorial plane defined by D_2, D_3 and D_4 and the proximity of the attacking nucleophile. Because there are large differences in atomic size of the various ligand atoms the compounds were grouped as (a) those containing at least two second-row-element atoms in the equatorial plane, and (b) those with two or more third-row (or greater) elements as equatorial ligands. We note that, in general, the compounds of group (b) correspond to those of class (i), while those of group (a) are mostly represented in class (iii). We calculated the weighted average interatomic distances, Zn-$D_{equatorial}$, for the two groups as 199 pm and 235 pm respectively, and obtained correlations by plotting d_1 and d_5 against z, as shown in Figs. 9(a) and 9(b). Following the method used by Bürgi (1973) in his analogous study of five-coordinate Cd complexes, we reflected the d_5 *vs* z plot across the line $z=0$ (as shown in Fig. 9b) in order to treat d_1 and d_5 as a single function of z so that $d_1=f(z)$ and $d_5=f(-z)$. The correlation figures show that as the nucleophile D_5 approaches the ZnL_4 tetrahedron at the face opposite the leaving groups D_1, the latter draws away from the Zn and the resulting ZnL_3 pyramid flattens. In the intermediate

$$\{D_5 \ldots ZnL_3 \ldots D_1\}$$

$z=0$, d_1 and d_5 are equal and have values of 12 pm and 26 pm for groups (a) and (b) respectively.

The data sets were fitted to the logarithmic curve

$$d_1,\ d_5 = f(\pm z) = a \log (\pm z + z_{max}) + b,$$

where z_{max} is the maximum out-of-plane displacement of the Zn atom from the plane $D_2D_3D_4$. This occurs when the attacking nucleophile D_5 is at an infinite distance from the ZnL_4 tetrahedron. The maximum displacements are calculated as 66 pm for group (a) and 79 pm for group (b).

Least-squares fit to the two data sets yielded:

$$\begin{aligned} &\text{group } (a) \quad d_1,\ d_5 = 106 - 52 \log (\pm z + 66) \\ &\text{group } (b) \quad d_1,\ d_5 = 294 - 141 \log (\pm z + 79). \end{aligned} \tag{1}$$

These were transformed to:

$$\begin{aligned} &\text{group } (a) \quad d_1,\ d_5 = -52 \log \{(\pm z + 66)/109\} \\ &\text{group } (b) \quad d_1,\ d_5 = -141 \log \{(\pm z + 79)/121\} \end{aligned} \tag{2}$$

in order to make direct comparison with Pauling's (1947) formula $d=-C \log n$ which describes the variation of interatomic distance increments d with bond number n. We thus obtain:

$$\begin{aligned} &\text{group } (a) \quad n_1,\ n_5 = (\pm z + 66)/109 \\ &\text{group } (b) \quad n_1,\ n_5 = (\pm z + 79)/121 \end{aligned} \tag{3}$$

$$\begin{aligned} &\text{group } (a) \quad n_1 + n_5 = 1{\cdot}2 \\ &\text{group } (b) \quad n_1 + n_5 = 1{\cdot}3. \end{aligned} \tag{4}$$

Therefore, the bond numbers vary linearly with z and their sum is constant at approximately unity. This implies that, as substitution proceeds, the D_5-Zn bond is created at the expense of the Zn-D_1 bond. The fact that $n_1+n_5>1$ may indicate d-orbital contribution to axial bonding.

Table 5. *Out-of-plane displacements* z (pm) *for t.b.p. and* x (pm) *for s.p. structures*

	z	x		z	x		z	x
(1)	−1	41	(13)	2	63	(24)	5	35
(2)	9	56	(14)	8	32	(25)	0	82
(3)	39	50	(15)	11	35	(26)	11	72
(4)	4	64	(16)	27	69	(27)	38	41
(5)	32	57	(17)	44	46	(28)	3	54
(6)	2	41	(18)	31	78	(29)	3	46
(7)	27	52	(19)	21	63	(30)	26	41
(8)	25	68	(20)	19	47	(31)	3	47
(9)	23	69	(21a)	43	29	(32)	1	56
(10)	5	39	(21b)	49	95	(33)	16	71
(11)	4	40	(22)	17	51			
(12)	35	63	(23)	33	53			

We failed to find any structural correlation for the square-pyramidally distorted structures. We sought a sequential change of the displacement x of the Zn atom out of the basal plane $D_1D_2D_4D_5$ with d_5 (Table 5) but found no convincing relation. Possibly the s.p. branch of the reaction coordinate mapped in Fig. 8 represents a *cul-de-sac* of the reaction pathway into which the compounds have been forced by intramolecular steric requirements or crystal packing forces or both.

The correlation between the axial distance increments d_1 and d_5 is shown in Fig. 10 for the compounds of group (b). The data were fitted to Pauling's equation $d=-C \log n$ where C is an empirical constant. Holding the sum of the bond orders n_1 and n_5 to the values obtained in equation (4) we obtain

$$10^{-d_1/C} + 10^{-d_5/C} = 1{\cdot}2;\ 1{\cdot}3, \tag{5}$$

which yields C values of 57 and 146 for groups (a) and (b) respectively.

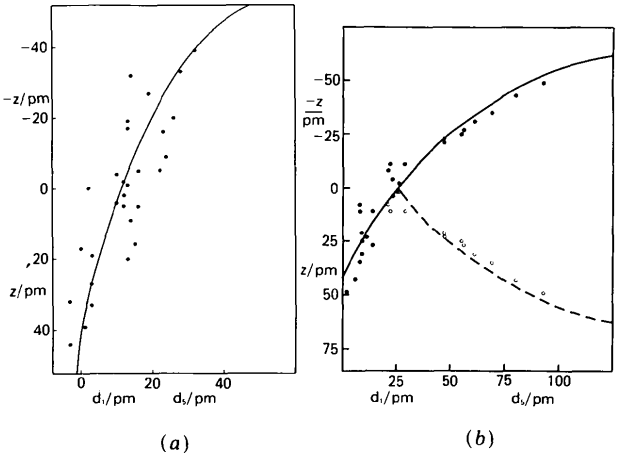

Fig. 9. (a), (b) Plot of displacement z of zinc from the equatorial plane *versus* distance increments d_1 and d_5 for groups (a) and (b) respectively as explained in the text.

Fig. 10 mirrors similar relationships found in other triatomic linear systems, both in the crystalline state (Bürgi, 1975) and in hypothetical systems such as the addition of an H atom to a hydrogen molecule H_2 to yield the linear system [H . . . H . . . H] (Liu, 1973).

In our model of the reaction,

$$D_5 + L_3ZnD_1 \rightarrow \{D_5 \ldots ZnL_3 \ldots D_1\} \rightarrow D_5ZnL_3 + D_1,$$

the intermediate is assumed to be that structure for which $d_1 = d_5$. The values of C were used to calculate d_1 and d_5 for $n_{1,5} = 0{\cdot}6$; $0{\cdot}65$ yielding distance increments of 13 pm for group (a) and 27 pm for group (b). These values are in close agreement with those obtained by putting $z = 0$ in equations (1).

The above discussion has focused on modelling the dynamics of the system. We have also considered the directional preferences of nucleophilic attack on the Zn^{2+} ion. Fig. 11 shows two possible approaches of the nucleophile to tetrahedral Zn. For an ideal 'face' approach, F, the nucleophile-Zn-ligand angles are 180° for θ_{15} and 70·5° for θ_{52}, θ_{53} and θ_{54}; while an edge approach, E, gives rise to two pairs of angles of 125·3 and 54·7°. A scatterplot of the angles subtended between D_5 and the $Zn(D)_4$ tetrahedra is shown in Fig. 12. This shows that the approach cannot be classified as either F or E, but as somewhere between. This is in agreement with the result obtained from Fig. 8, which shows that the conformations at the early stage of reaction ($d_5 > 30$ pm) are displaced approximately 57% towards s.p. Examination of Table 2 shows that, on average, the nucleophilic attack is inclined away from D_3 ($\langle\theta_{53}\rangle = 92{\cdot}9$, $\langle\theta_{52}\rangle = 83{\cdot}6$, $\langle\theta_{54}\rangle = 81{\cdot}7$°). We note that D_3 acts as pivot for the Berry pseudorotation but this could be simply due to the nomenclature we employed.

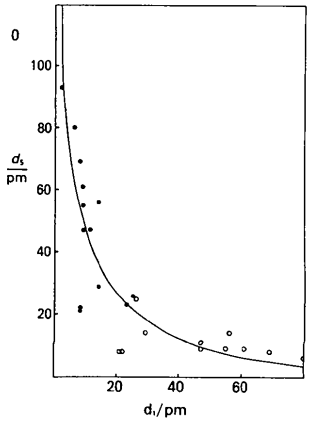

Fig. 10. Correlation between axial distance increments d_1 and d_5.

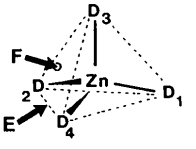

Fig. 11. Geometry of nucleophilic attack showing face approach F, and edge approach E.

Experimental observations

The correlations derived are consistent with a substitution reaction at tetrahedral Zn *via* an S_N2 mechanism, and a possible Berry pseudorotation of the five-coordinate intermediate.

Experimental evidence which supports this is comparatively recent (Barefield & Wagner, 1973; Lindoy & Busch, 1974; Dei, 1975; Neves & Dabrowiak, 1976). For the reaction of bis(μ-*N*,*N*-dibutyldithiocarbamato)zinc(II) with iodine in cyclohexane, the pentacoordinate intermediate shown in Fig. 13 has been proposed (Kita, Tanaka & Tanaka, 1977). Bis(*O*-ethyl xanthato)pyridinezinc(II), which has been used in this study (complex 25), has been proposed as lying along the reaction coordinate of the reaction

$$Zn(exa)_2 + L \rightleftarrows Zn(exa)_2L,$$

where exa = *O*-ethyl xanthato (= *O*-ethyl dithiocarbamato), L = py, EtOH, $(CH_3)_2CO$, Me_2SO.

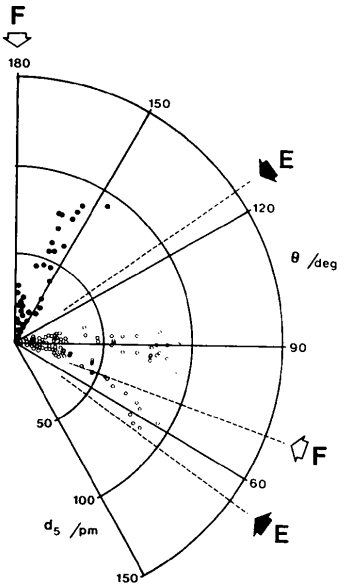

Fig. 12. Scatterplot showing angle of nucleophilic attack *versus* distance increment of nucleophile. Filled circles represent d_5 *vs* θ_{15}, open circles d_5 *vs* θ_{52}, θ_{53} and θ_{54}.

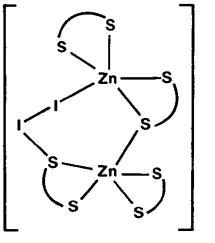

Fig. 13. Proposed intermediate for reaction of bis(μ-*N*,*N*-dibutyldithiocarbamato)zinc(II) with iodine.

Pentacoordinated intermediates have also been proposed for a number of biochemical reactions. In the enzyme-catalysed reversible hydration of carbon dioxide by carbonic anhydrase, the intermediate shown in Fig. 14 has been suggested (Gupta & Pesando, 1975; Kannan, Pelef, Fridborg, Cid-Dresner & Lövgren, 1977). A pentacoordinate intermediate has also been proposed in the catalytic cycle involving alcohol dehydrogenase and nicotinamide coenzyme (Dworschach & Plapp, 1977), while a general examination of the active-site geometries of Zn enzymes has been undertaken (Argos, Garavito, Eventoff, Rossmann & Branden, 1978). In all cases the metal ion is bonded by three protein ligands and water in a distorted tetrahedral arrangement, and it is suggested that the substrate may bind at a fifth coordination site.

The labile nature of Zn–thiourea complexes in solution has been examined (Eaton & Zaw, 1976) and the ligand exchange has been found to occur *via* an associative mechanism. Such a bimolecular ligand-exchange mechanism has also been proposed for thiocumatozinc(II) derivatives (Fackler & Fetchin, 1970). One of the proposals advanced to explain the acetate scrambling process in the *meso*-2,3-tetramethylenediaminetetraacetic acid complex with zinc(II) involves a pentacoordinate intermediate of either t.b.p. or s.p. conformation (Mirti, Gennaro & Vallinotto, 1982). The addition of sulphur to dithiobenzoato complexes of zinc(II) has been studied, with the conclusion that the mechanism of the reaction involves addition of an S atom and a subsequent rearrangement of the ligands about the Zn (Fackler, Fetchin & Fries, 1972). Interestingly, there is also a report of a fluxional pentacoordinate Zn complex (Alcock, Herron & Moore, 1978). A ^{13}C NMR investigation has been carried out on the complex $[ZnXL]^+$ in nitromethane (X = halide, NCS^- or ClO_4^-; L is a quadridentate methyl-substituted tetraazacyclotetradecane ligand). A dynamic process which possibly involves the interconversion of axial and equatorial *N*-methyls, *via* a Berry mechanism, is indicated as shown in Fig. 15. This complex was used in our study, compound (28).

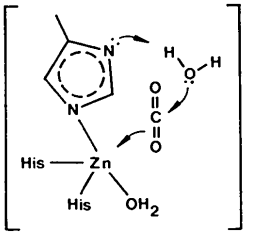

Fig. 14. Proposed intermediate for hydration of CO_2 by carbonic anhydrase.

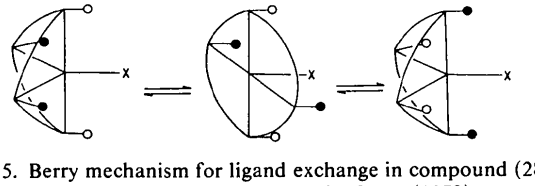

Fig. 15. Berry mechanism for ligand exchange in compound (28). Adapted from Alcock, Herron & Moore (1978).

While the structural-correlation principle can only yield indirect information of the reaction path and the transition state, it is gratifying that in the case of reactions of zinc(II), solution and solid-state data are compatible.

We thank the University of Cape Town and CSIR (Pretoria) for research grants.

References

ALCOCK, N. W., HERRON, N. & MOORE, P. (1978). *J. Chem. Soc. Dalton Trans.* pp. 1282–1288.

ALTMANN, J. A., YATES, K. & CSIZMADIA, I. G. (1976). *J. Am. Chem. Soc.* **98**, 1450–1454.

ARCHER, S. J., MODRO, T. A. & NASSIMBENI, L. R. (1981). *Phosphorus Sulfur*, **11**, 101–110.

ARGOS, P., GARAVITO, R. M., EVENTOFF, W., ROSSMANN, M. G. & BRANDEN, C. I. (1978). *J. Mol. Biol.* **126**, 141–158.

BAREFIELD, E. K. & WAGNER, F. (1973). *Inorg. Chem.* **12**, 2435–2439.

BASOLO, F. & PEARSON, R. G. (1967). *Mechanisms of Inorganic Reactions*, p. 438. New York: John Wiley.

BERRY, R. S. (1960). *J. Chem. Phys.* **32**, 933–938.

BRITTON, D. & DUNITZ, J. D. (1981). *J. Am. Chem. Soc.* **103**, 2971–2979.

BÜRGI, H. B. (1973). *Inorg. Chem.* **12**, 2321–2325.

BÜRGI, H. B. (1975). *Angew. Chem.* **14**, 460–473.

BÜRGI, H. B., DUNITZ, J. D., LEHN, J. M. & WIPFF, G. (1974). *Tetrahedron*, **30**, 1563–1572.

BÜRGI, H. B., DUNITZ, J. D. & SHEFTER, E. (1974). *Acta Cryst.* B**30**, 1517–1527.

BYE, E. SCHWEIZER, W. B. & DUNITZ, J. D. (1982). *J. Am. Chem. Soc.* **104**, 5893–5898.

DEI, A. (1975). *Inorg. Chim. Acta*, **12**, 79–83.

DUNITZ, J. D. (1979). *X-ray Analysis and the Structure of Organic Molecules*, chs. 7–10. Ithaca: Cornell Univ. Press.

DWORSCHACH, R. T. & PLAPP, B. V. (1977). *Biochemistry*, **16**, 2716–2725.

EATON, D. R. & ZAW, K. (1976). *J. Inorg. Nucl. Chem.* **38**, 1007–1010.

FACKLER, J. P. & FETCHIN, J. A. (1970). *J. Am. Chem. Soc.* **92**, 2912–2913.

FACKLER, J. P., FETCHIN, J. A. & FRIES, D. C. (1972). *J. Am. Chem. Soc.* **94**, 7323–7333.

FAVAS, M. C. & KEPERT, D. L. (1980). *Prog. Inorg. Chem.* **27**, 325–463.

GUPTA, R. K. & PESANDO, J. M. (1975). *J. Biol. Chem.* **250**, 2630–2634.

HOLMES, R. R. (1979). *Acc. Chem. Res.* **12**, 257–265.

KANNAN, K. K., PELEF, M., FRIDBORG, K., CID-DRESNER, M. & LÖUGREN, S. (1977). *FEBS Lett.* **73**, 115–119.

KENNARD, O., WATSON, D. G., ALLEN, F. H., MOTHERWELL, W. D. S., TOWN, W. G. & RODGERS, J. (1975). *Chem. Br.* **11**, 213–216.

KITA, H., TANAKA, K. & TANAKA, T. (1977). *Inorg. Chim. Acta*, **21**, 229–232.

LINDOY, L. F. & BUSCH, D. H. (1974). *Inorg. Chem.* **13**, 2494–2498.

LIU, B. (1973). *J. Chem. Phys.* **58**, 1925–1937.

MIRTI, P., GENNARO, M. C. & VALLINOTTO, M. (1982). *Trans. Met. Chem.* **7**, 2-5.
MUETTERTIES, E. L. & GUGGENBERGER, L. J. (1974). *J. Am. Chem. Soc.* **96**, 1748-1756.
NEVES, D. R. & DABROWIAK, J. C. (1976). *Inorg. Chem.* **15**, 129-134.
PAULING, L. (1947). *J. Am. Chem. Soc.* **69**, 542-553.
RUSSEGGER, P. & BRICKMANN, J. (1975). *Chem. Phys. Lett.* **30**, 276-278.
UGI, I., MARQUARDING, D., KLUSACEK, H., GILLESPIE, P. & RAMIREZ, F. (1971). *Acc. Chem. Res.* **4**, 288-296.

Acta Cryst. (1984). B**40**, 590-595

Relation between Bonding and the Substitution-Dependent Geometry of a Number of Dicobalt Hexacarbonyl Acetylene Complexes

BY F. BAERT AND A. GUELZIM

Laboratoire de Dynamique des Cristaux Moléculaires, Associé au CNRS (n° 465), Université des Sciences et Techniques de Lille, 59655 Villeneuve d'Ascq CEDEX, France

AND P. COPPENS

Department of Chemistry, State University of New York at Buffalo, Buffalo, NY 14214, USA

(*Received* 24 *February* 1984; *accepted* 13 *June* 1984)

Abstract

The molecular structures of five dicobalt hexacarbonyl acetylene complexes, $Co_2(CO)_6(R\text{-}C{\equiv}C\text{-}R)$, are analyzed in terms of variation in their geometry as a function of increasing electronegativity of the substituent R. The crystal structures of three of the five complexes with $R = COOH$, CH_2OH and CF_3 have been determined for the first time and are reported. Crystal data are as follows: $R = COOH$: $[Co_2(CO)_6(C_4H_2O_4)]$, $M_r = 400{\cdot}0$, $P2_12_12_1$, $a = 7{\cdot}059\ (2)$, $b = 11{\cdot}107\ (3)$, $c = 17{\cdot}516\ (5)$ Å, $Z = 4$, $V = 1373{\cdot}3$ Å^3, $D_m = 1{\cdot}80$-$2{\cdot}00$, $D_x = 1{\cdot}93$ g cm^{-3}, Mo $K\bar{\alpha}$, $\lambda = 0{\cdot}7107$ Å, $T = 293\ (2)$ K; $R = CH_2OH$ (monohydrate): $[Co_2(CO)_6(C_4H_6O_2)].H_2O$, $M_r = 390{\cdot}0$, $P2_1/c$, $a = 7{\cdot}974\ (3)$, $b = 12{\cdot}591\ (5)$, $c = 14{\cdot}551\ (6)$ Å, $\beta = 104{\cdot}31\ (5)°$, $Z = 4$, $V = 1415{\cdot}6$ Å^3, $D_m = 1{\cdot}80$-$2{\cdot}00$, $D_x = 1{\cdot}83$ g cm^{-3}, Mo $K\bar{\alpha}$, $T = 293\ (2)$ K; $R = CF_3$: $[Co_2(CO)_6(C_4F_6)]$, $M_r = 448{\cdot}0$, $P2_1/c$, $a = 7{\cdot}538\ (3)$, $b = 30{\cdot}804\ (9)$, $c = 12{\cdot}681\ (6)$ Å, $\beta = 100{\cdot}49\ (4)°$, $Z = 8$, $V = 2895{\cdot}4$ Å^3, $D_m = 1{\cdot}95$-$2{\cdot}10$, $D_x = 2{\cdot}05$ g cm^{-3}, Mo $K\bar{\alpha}$, $T = 100\ (0{\cdot}5)$ K. Final $R(F)$ factors are 2·8, 4·8 and 5·2% respectively. The two other complexes discussed here with $R = Ph$ and $R = C(CH_3)_3$ have been reported recently by Gregson & Howard [*Acta Cryst.* (1983), C**39**, 1024-1027]. The metal-acetylenic ligand distances decrease with increasing electronegativity of R, while the acetylenic C-C distance increases, indicating the strengthening of the $Co\text{-}C_{ac}$ bonds to be due to increased back donation. The effect is attributed to a stabilization of the ligand a_2 and b_1 orbitals by the electronegative substituents. Various correlations between geometric distortion parameters are discussed.

Introduction

There is considerable interest in the study of polynuclear complexes because of their relevance as model compounds for metal-catalyzed reactions such as hydrogenation and carbonylation. As the attachment of a single molecule to more than one metal atom is related to the bonding of an organic substrate to a metal surface, the detailed study of such model compounds is of importance. Complexes of the type studied here may also be regarded simply as possible intermediates in homogeneous catalytic reactions.

The present study is part of a series of investigations on the effect of metal-ligand bonding on ligand geometry and ligand electron distribution. Studies on dicobalt octacarbonyl (Leung & Coppens, 1983) and methylidynetricobalt nonacarbonyl (Leung, 1983) have been reported.

We report here on the geometry of three dicobalt hexacarbonyl acetylenes with general formula $Co_2(CO)_6(R\text{-}C{\equiv}C\text{-}R)$ and their comparison with two complexes of this type determined by Gregson & Howard (1983). The choice of the radical R was guided by two considerations. A range of electronegativities was desired to enable the detection of substitution-related trends in geometry and electron distribution. In addition we have avoided H atoms as much as possible to eliminate the need for neutron diffraction data in the electron density studies.

Experimental

Synthesis

All manipulations were performed in a dry nitrogen gas atmosphere.

0108-7681/84/060590-06$01.50